



PERGAMON

Vacuum 58 (2000) 149–157

VACUUM

SURFACE ENGINEERING, SURFACE INSTRUMENTATION  
& VACUUM TECHNOLOGY

www.elsevier.nl/locate/vacuum

# Electron transport in high- $T_c$ superconducting grain boundary junctions<sup>☆</sup>

Gennady A. Ovsyannikov\*, Igor V. Borisenko, Karen Y. Constantinian

*Institute of Radio Engineering and Electronics RAS, Moscow 103907, Russia*

## Abstract

The current state and the prospects of the application of high- $T_c$  superconducting grain boundary Josephson junctions in microwave electronics devices are given. It is approached by sketching the typical fabrication technique of the junction. Josephson bicrystal junctions on sapphire substrate are considered in detail. The results of dc microwave and magnetic measurements of YBCO bicrystal junctions on r-cut sapphire are presented. The junctions with high resistance 10–20  $\Omega$  and  $I_c R_N = 1$ –2 mV and tolerance of  $R_N S$  around 30% on the chip allow to create microwave circuits with low integration (up to 10 junctions on chip). The microwave dynamics of the junction with superconducting current-phase relation fits with  $\sin\varphi$  relation better than 5%, that clearly indicates the tunnel conductivity between two YBCO electrodes. It was found that critical current density depends on the square root of interface transparency in accordance with the prediction of superconducting current transport via Andreev's bound surface states. The specific properties of current transport in high- $T_c$  grain boundary junctions with taking into account d-wave type of gap order in high- $T_c$  superconductor are discussed. © 2000 Elsevier Science Ltd. All rights reserved.

*Keywords:* High- $T_c$  superconductivity; Josephson bicrystal junctions; Andreev's states; Current transport

## 1. Introduction

Low- $T_c$  superconducting electronics is based on the three-layers structure, superconductor–insulator–superconductor (SIS) tunnel junction Nb/Al<sub>2</sub>O<sub>3</sub>/Nb with the tolerance of parameters (critical current and normal resistance) 2–5% on chip (see for example Ref. [1]). Specific

<sup>☆</sup>Paper presented at the 11th International School on Vacuum, Electron and Ion Technologies, 20–25 September 1999, Varna, Bulgaria.

\* Corresponding author. Tel.: + 7095-203-0935; fax: + 7095-203-8414.

E-mail address: gena@lab235.cplire.ru (G.A. Ovsyannikov).

properties of high- $T_c$  material like low coherence length, strong anisotropy and sensitivity to oxygen deficiency make the three-layers structure fabrication difficult. Surface quality for three-layer high- $T_c$  superconducting structure should be 1–2 order better than for low- $T_c$  one. So nontraditional for low- $T_c$  superconducting electronics approach, grain-boundary junction technology, is often used in high- $T_c$  superconducting devices. The experimentally established appearance of weak link coupling between two grains, with the crystallographic axis misoriented on angle  $\alpha$ , is applied for realization of grain boundary junctions. Depending on the fabrication technique, the grain-boundary junctions are distinct into bicrystal, biepitaxial and step-edge junctions [2].

The high values of normal-state resistance  $R_N$  and critical frequency  $f_c = (2e/h)I_c R_N$ , as well as the absence of hysteresis on the  $I$ – $V$  curve of high- $T_c$  superconducting (HTSC) Josephson junctions even at liquid-helium temperature  $T = 4.2$  K, make them appreciably superior to low-temperature superconducting junctions. The high critical temperature gives promising opportunities for applications at frequencies higher than those, corresponding to the energy gap of an ordinary (say, Nb) superconductor. However, the aspects involved in the reproducible fabrication of high-quality HTSC Josephson junctions on one hand, and the mechanism, describing current transport, on the other hand are the problems which have not been solved yet. The most reproducible junctions having a critical current spread of  $\pm 12\%$  per chip are fabricated on SrTiO<sub>3</sub> bicrystal substrates [3], but because of their high dielectric constant  $\varepsilon > 1000$ , they are unsuitable for high-frequency applications. Sapphire having a relatively low  $\varepsilon \approx 9$ –11 and low losses ( $\tan \delta \approx 10^{-8}$  at 72 GHz), is the traditional material used in microwave electronics [3–5]. Here, we present the results of fabrication and characterization of HTSC Josephson junctions on sapphire bicrystal substrates both at DC and microwaves. The model based on the contact of d-wave superconductors is used for description of the electron transport mechanism in a bicrystal junction.

## 2. Experimental

### 2.1. Fabrication technique

The Josephson junctions were fabricated on the r-cut sapphire bicrystal substrates (crystallographic plane  $(1\ \bar{1}\ 0\ 2)$  Al<sub>2</sub>O<sub>3</sub>) consisting of two crystals for which the directions  $\langle 1\ 1\ \bar{2}\ 0 \rangle$  Al<sub>2</sub>O<sub>3</sub> for both parts were misoriented at the angles  $\pm 12^\circ$  to the plane of the interface. The YBa<sub>2</sub>Cu<sub>3</sub>O<sub>x</sub> (YBCO) film was grown at  $T = 750$ – $770^\circ\text{C}$  by dc sputtering (in diode configuration) at high oxygen pressure (4 mbar) after the CeO<sub>2</sub> epitaxial buffer layer rf magnetron sputtering at  $T = 600$ – $750^\circ\text{C}$  and pressure 0.01 mbar in an Ar/O<sub>2</sub> mixture. The CeO<sub>2</sub> buffer layer prevents Al atoms diffusing into the YBCO film from the substrate. The following epitaxial relation  $(0\ 0\ 1)\text{YBCO} // (0\ 0\ 1)\text{CeO}_2 // (1\ \bar{1}\ 0\ 2)\text{Al}_2\text{O}_3$ ,  $\langle 1\ 1\ 0 \rangle\text{YBCO} // \langle 0\ 0\ 1 \rangle\text{CeO}_2 // \langle 1\ 1\ \bar{2}\ 0 \rangle\text{Al}_2\text{O}_3$ , was fulfilled for the deposited films (Fig. 1). Thin-film YBCO bridges each 5  $\mu\text{m}$  wide and 10  $\mu\text{m}$  long, crossing the bicrystal boundary, were initially formed by rf plasma etching of the upper amorphous CeO<sub>2</sub> layer which acts as a mask. YBCO was then subjected to liquid chemical etching in 0.5% ethanol solution of Br<sub>2</sub> through the CeO<sub>2</sub> mask [5]. We have made the samples in which the YBCO bridges crossed the boundary at the angle  $\gamma$  between the normal to the boundary interface and current direction varied from 0 to  $54^\circ$  (see Fig. 1).

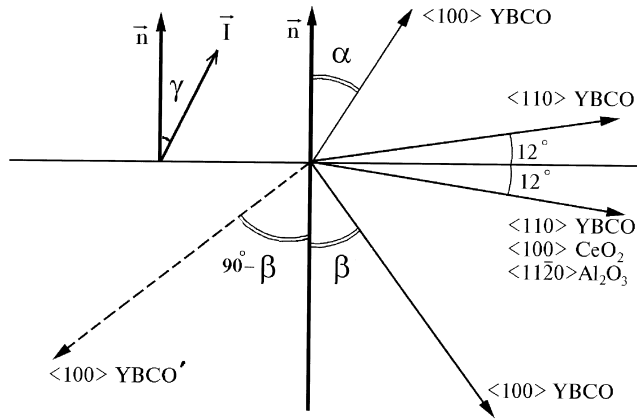


Fig. 1. Crystallographic axes orientations of  $\text{CeO}_2$  and YBCO films in sapphire bicrystal junction with  $\alpha = 33^\circ$ ,  $\beta = -33^\circ (D_{33}ID_{-33})$ . The domain of the film with the direction  $\langle 100 \rangle \text{YBCO}$  misoriented on the angle  $\beta = 90^\circ - \beta$  is the twin to YBCO.

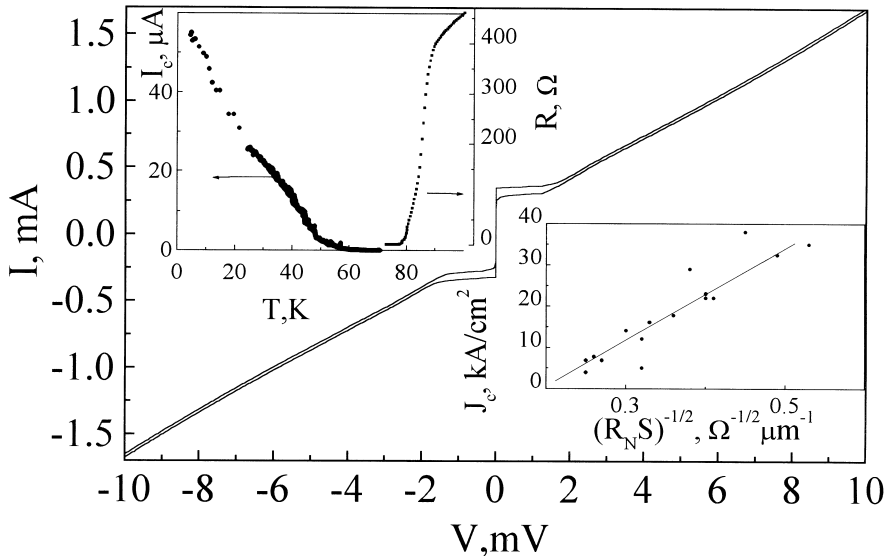


Fig. 2. The  $I$ - $V$  curve at  $T = 4.2$  K for a typical bicrystal junction. Temperature dependence of the resistance  $R(T)$  and critical current  $I_c(T)$  are shown in the left inset. Dependence of the critical current density vs. inverse square root of characteristics interface resistance at  $T = 4.2$  K is shown in the right inset.

## 2.2. DC measurement results

The junctions with current density  $10^4$ – $10^5$  A/cm<sup>2</sup>  $V_0 = I_c R_N = 0.5$ – $2$  mV at  $T = 4.2$  K were obtained. The typical  $I$ - $V$  curve of the junction is shown in Fig. 2. It obviously demonstrates a behavior very close to the resistive shunted junction (RSJ) model which has two channels for current: quasiparticle  $V/R_N$  and superconducting  $I_s(\varphi) = I_c \sin \varphi$ . Very small (or even negative)

excess current on the  $I$ – $V$  curve at  $V > 10$  mV points to the absence of channels with direct (nontunnel) conductivity. However,  $I_c(T)$  function shown in the inset of Fig. 2, has a linear temperature dependence which distinguishes it from the known theoretical one for superconductor–insulator–superconductor junctions [6]. At  $T_c - T < T_c$ , where the influence of thermal fluctuation is strong,  $I_c(T)$  is close to  $(T_c - T)^{1/2}$  dependence.  $I_c(T)$  is possibly depressed by either the existence of the layer with depressed gap or by the specifics of proximity effect in d-wave superconductors [6,7].

The critical temperature of base electrode of the junction is in the range 86–88 K. We observe a significant reduction of junction resistance in this temperature range.  $R(T)$  has a foot-like temperature dependence at lower  $T$  with a plateau equal to the normal resistance of the junction  $R_N$ . The plateau of constant resistance takes place, when the YBCO film on both sides of the step is already in the superconducting state. We think that the two processes determine appearance of plateau. The first one is Al diffusion and second is the temperature fluctuation.

The following formula has been used for determination of barrier transparency  $\bar{D}$ :

$$\bar{D} = 2\rho^{\text{YBCO}}1^{\text{YBCO}}/(3R_N S), \quad (1)$$

where  $\rho^{\text{YBCO}}1^{\text{YBCO}} \approx 3.2 \times 10^{-11} \Omega \text{ cm}^2$  for YBCO. For typical  $R_N S = 5 \times 10^{-8} \Omega \text{ cm}^2$ , we obtained  $\bar{D} = 4 \times 10^{-3}$ . The bottom inset of Fig. 2 shows the current density dependence  $j_c = I_c/S$  from  $R_N S$ . The experimentally obtained dependence is proportional to  $j_c \propto (R_N S)^{-1/2} \propto \sqrt{\bar{D}}$  is unusual for junctions of s-superconductors. Typically,  $j_c \propto \bar{D}$  for SIS junction [6].

### 2.3. Current–phase relation

Current–phase relation  $I_S(\varphi)$  strongly depends on the type of contacts between superconductors. For  $T_c - T \ll T_c$  the deviations of  $I_S(\varphi)$  from  $I_S(\varphi) = I_c \sin \varphi$  are small for any type of superconducting junction, but at  $T \ll T_c$   $I_S(\varphi) = I_c \sin \varphi$  remains for SIS junction [6] regardless of the transparencies of the barrier  $\bar{D} \ll 1$ . To estimate deviation from  $I_S(\varphi) = I_c \sin \varphi$  we have measured  $I$ – $V$  curves under applied monochromatic mm wave radiation  $A \sin(2\pi f_e t)$ ,  $f_e = 40$ – $100$  GHz [5]. The Shapiro steps on  $I$ – $V$  curves, observed at voltages corresponding to the harmonics of the microwave frequency, demonstrate the presence of Josephson coupling in the junctions. Fig. 3 shows the variation of  $I_1(A)$  and subharmonic Shapiro step  $I_{1/2}(A)$  for two junctions with  $\gamma = 0$  (symmetrical biasing) and  $\gamma = 54^\circ$  (nonsymmetrical one). The calculated functions using RSJ model for  $f_e > 2eI_c R_N/h$  in the case of  $I_S(\varphi) = I_c \sin \varphi$  and  $I_S(\varphi) = (1 - \delta)I_c \sin \varphi + \delta I_c \sin 2\varphi$  at  $\delta = 0.2$  are presented in Fig. 3. For  $\delta < 1$ , the difference between these two theoretical dependencies of  $I_c(P_e)$  is small and both cases fit well to experiment. At the same time, a small deviation  $I_S(\varphi)$  from sin-type dependence yields subharmonic (fractional  $n/m$ ) Shapiro steps. The maximum amplitude of subharmonic steps  $I_{m/n}$  are proportional to harmonics  $\sin(n\varphi)$  in  $I_S(\varphi)$ . The precise measurements of  $I_n(A)$ , as well as  $I_{m/n}(A)$  at  $T = 4.2$  K ( $T/T_c \approx 0.05$ ) allow us to state the absence of  $\sin(2\varphi)$  components in  $I_S(\varphi)$  function for BJ with symmetrical biasing ( $\gamma = 0 \div 36^\circ$ ) with an accuracy of at least 5%. For  $\gamma > 40^\circ$   $\delta$  increases monotonously.

So quite high junction resistance (10–20  $\Omega$ ), characteristic voltage  $I_c R_N = 1$ – $2$  mV and tolerance of  $R_N S$  around 30% on chip allow to realize microwave circuits with small integration of junctions on chip. The microwave dynamics of the junction with superconducting current–phase relation fits

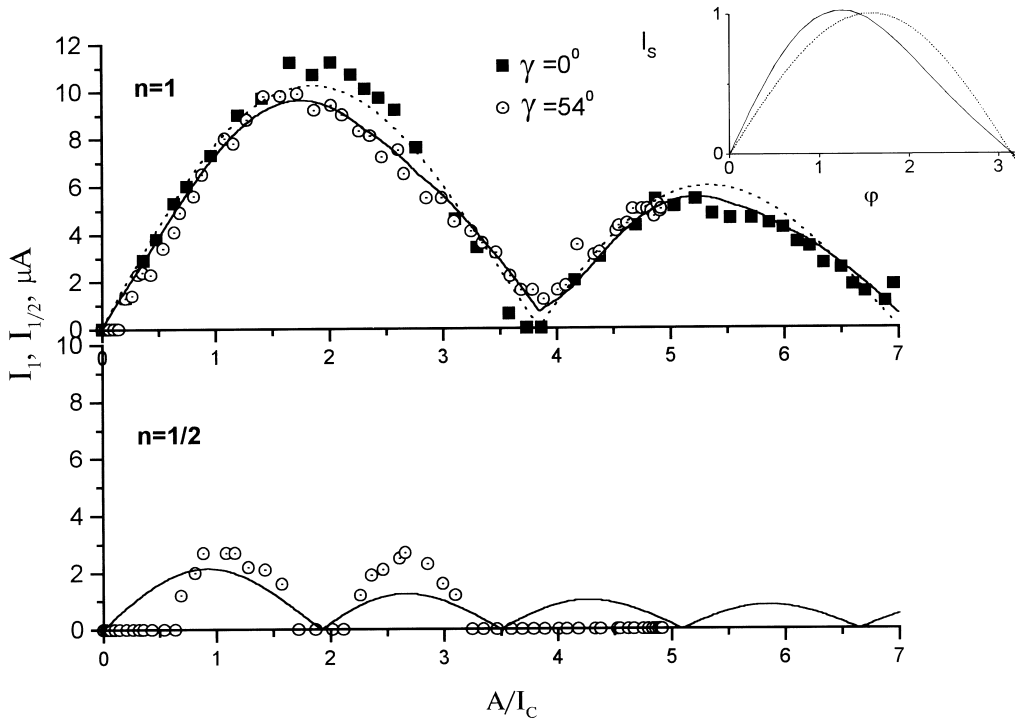


Fig. 3. Normalized RF current dependence of the first and half Shapiro steps for two BJ  $\gamma = 0$  (crosses), and  $\gamma = 54^\circ$  (filled circles). Dashed and solid lines show the calculated curves for  $\delta = 0$  and  $0.2$ , respectively. The current–phase relations for these two cases are shown in the inset.

with  $\sin \phi$  relation better than 5%, which prevents any parasitic effect in these Josephson device operations.

### 3. Discussion

#### 3.1. Andreev's states in Josephson junctions

It has been shown [8–10] that the transfer of copper pairs (superconducting Josephson current) is a complex process which takes place via an “intermediate” electron–hole state, where superconducting pairs are dissolved. The states are caused by Andreev's reflection and realize at the border between two superconductors with different superconducting phases. The induced Andreev reflection energy levels are responsible for superconducting current transferring through the normal layer. Each time an electron is Andreev reflected into a hole, a Cooper pair is effectively generated. Therefore the state, which represents an infinite loop of Andreev reflections (electron–hole–electron) serves as a pump that transfers Cooper pairs from one superconductor to the other. The states localized in the interlayer in the junction with direct conductivity (SNS, ScS junction,  $N$ -normal metal interlayer,  $c$ -constriction) and at the distance  $l_0 \approx \xi_0 \Delta / \sqrt{(\Delta^2 - E^2)}$  in the vicinity of the

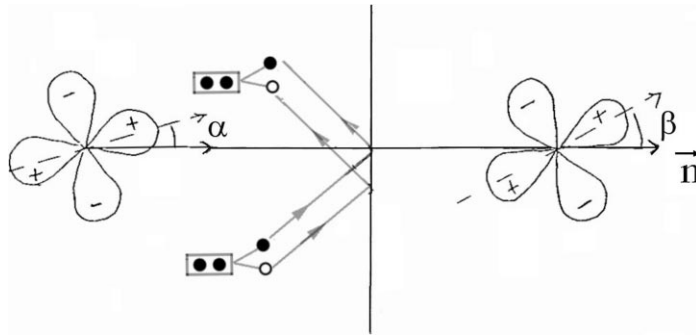


Fig. 4. Scheme of Andreev's reflection in a high- $T_c$  bicrystal junction.

interface in SIS junctions. Finally, in all types of superconducting junctions (SNS, ScS and SIS) Andreev's levels describe the formula

$$E_B = \pm \Delta \sqrt{(1 - \bar{D} \sin^2 \varphi/2)}. \quad (2)$$

The levels are placed close to the gap in tunnel junction with small transparency of the barrier ( $\bar{D} \ll 1$ ) and the particularities induced by it is weak as observed from the experiments. Most of the properties of SIS junctions are well described by the tunnel Hamiltonian model [6].

### 3.2. Andreev's states in d-wave Josephson junctions

The influence of Andreev's state is strong in SNS (ScS) junction ( $\bar{D} \approx 1$ ) or in superconducting tunnel junction with nontrivial superconducting pairing, for example d-wave superconductor. For SNS junction Andreev's levels give other than in SIS junction absolute value and temperature dependence of critical current and nonsinusoidal current–phase relation at low  $T$  [7,8].

A superconducting order parameter with d-wave symmetry changes sign in  $a$ - $b$  plane, when rotated by  $90^\circ$  around the  $c$ -axis. Since a quasiparticle changes its momentum when scattered, and there is a slight difference of order parameter before and after scattering, a bound state appears. An electron travelling towards the surface of d-wave superconductor, which is not parallel to a crystal axis, is reflected back into d-wave superconductor and is subsequently Andreev reflected into the hole by the positive pair potential. In the next step, the hole follows the same path backwards, reflected at the surface, and is finally Andreev-reflected into another electron by negative pair potential. The surface of d-wave superconductor plays the role of point contact with  $\bar{D} = 1$  and the sign change in the pair potential corresponds to the phase difference  $\pi$  (Fig. 4). It is the essential physical difference between s-wave and d-wave tunnel Josephson junctions, the position of Andreev's level when the phase difference across the junction is zero. For the junction of d-wave superconductors the Andreev energy level is very close to the Fermi level and for s-wave, the energy is close to the gap. These localized midgap energy states opened additional channels for the current leading to the peak for conductivity in DIN junction [11] and to anomalous low-temperature variation of the superconducting current when the orientation angle of the d-wave order parameter is such that the midgap states form in the junction (the angle between a(b)-axis and normal to the border is in the range  $10$ – $45^\circ$ ) [10,12].

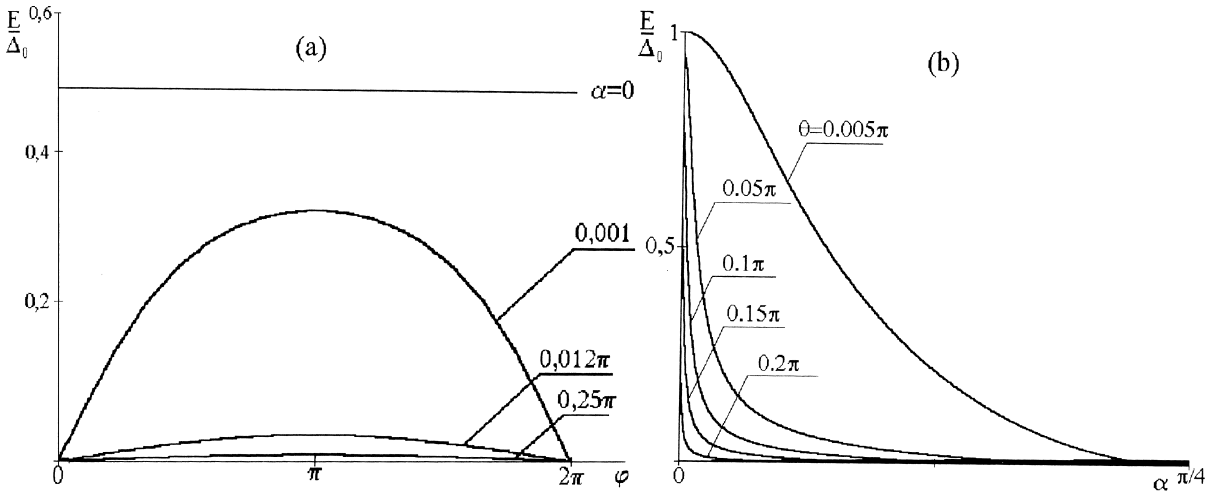


Fig. 5. (a) Andreev's levels in  $D_x I D_{-\alpha}$  junction for several  $\alpha$ ,  $\bar{D} = 10^{-4}$ ,  $\theta = \pi/6$ .  $E_B(\varphi)$  coincide with Eqs. (1) and (2) for  $\alpha = 0$  and  $\pi$ , respectively with proper  $\Delta(\theta)$ , (b) Amplitude of Andreev's levels in  $D_x I D_{-\alpha}$ ,  $\bar{D} = 10^{-4}$  for several  $\theta$ .

For the tunnel junction of two  $d_{x^2-y^2}$ -wave superconductors with gaps  $\Delta_{R(L)} = \Delta_0 \cos(2\theta + 2\alpha(\beta))$   $E_b$  depends on four angles, quasiparticle incident angle- $\theta$ , phase- $\varphi$  and, misorientation angles  $\alpha$  and  $\beta$ . Andreev levels for mirror symmetric junctions ( $D_x I D_{-\alpha}$ ) at several  $\alpha$  are presented in Fig. 5a. One can see that in the range  $\alpha = 10\text{--}45^\circ$   $E_b(\varphi)$ , dependence is very close  $E_B$  for misorientation angle  $\alpha = 45^\circ$

$$E_B = \pm \Delta(\theta) \cos[(\varphi - \pi)/2] \sqrt{\bar{D}(\theta)}. \quad (3)$$

The behavior of the amplitude of the Andreev levels with increasing  $\alpha$  at several incidence angles ( $\theta$ ) is shown in Fig. 5b. For  $\alpha = 10\text{--}45^\circ$  for a small amount of quasiparticle in the range  $\theta = 0\text{--}10^\circ$  the condition  $\max|E_B| > 0.1\Delta_0$  is satisfied. Therefore, the averaged income of these quasiparticles would be small. We can use as an approximation the Eq. (3) for describing Andreev's level in  $D_x I D_{-\alpha}$  junction in the wide range of  $\alpha = 10\text{--}45^\circ$ .

### 3.3. Determination of superconducting current using Andreev's levels

The  $I_S(\varphi)$  can be determined from the energy of bound Andreev levels  $E_B$  in the junction since  $I_S(\varphi) \propto dE_B/d\varphi$  [10,13]. The difference in  $E_B(\varphi)$  leads to other temperature and transparency dependence of critical current. In accordance with d-wave theory of superconducting junctions (DID) [10,12,13], various non-linear  $I_C(T)$  dependencies caused by the existence of bound states at the interface should be observed. Our measurements, as well as some other published data [14] instead show a monotonous (smooth) rise of  $I_C$  with decreased  $T$ . However, there are several physics phenomena, influencing the  $I_C(T)$ , which have not been accounted for in the theory. The first one is the twinning of the film, meaning that the current through the junction consists of two

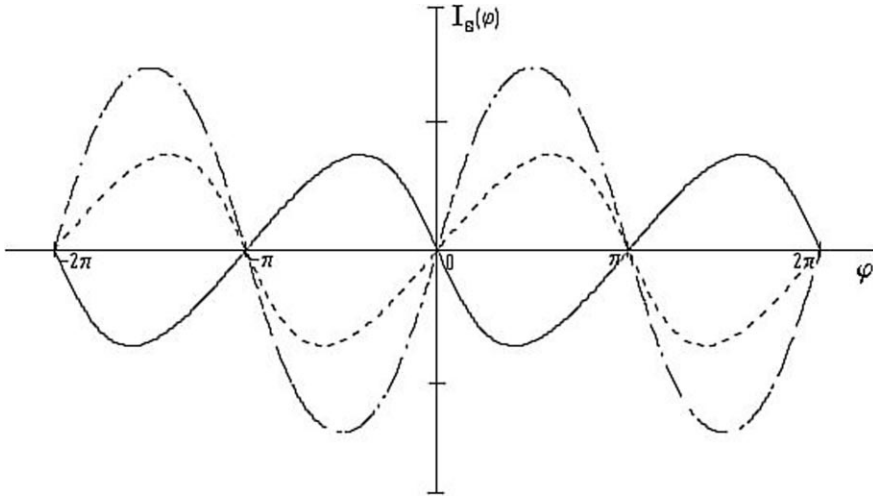


Fig. 6. Current–phase relation calculated for symmetrical ( $45^\circ, 45^\circ$ )-dotted line and mirror symmetrical ( $45^\circ, -45^\circ$ )-solid line bicrystal junctions. The dashed line corresponds to the parallel connection of these two junctions.

components: from mirror symmetrical junction (MSJ,  $D_\alpha ID_{-\alpha}$ ) and additional symmetrical junction (ASJ,  $D_\alpha ID_{90-\alpha}$ ), in our experiment  $D_{33} ID_{-33}$  and  $D_{33} ID_{57}$ . There is an essential difference between MSJ and ASJ, MSJ possesses the properties of  $\pi$ -contact and ASJ is 0-contact. Since  $E_B$  for misorientation angles in the range  $10$ – $45^\circ$  is very close to  $E_B$  for misorientation angles  $45^\circ$ , (Eq. (2)) we will compare our experimental data with the results of  $I_s(\varphi)$  calculation for symmetrical and mirror symmetrical junction with a misorientation of  $45^\circ$  (Fig. 6). As calculated  $I_s(\varphi)$  for  $D_{45} ID_{-45}$  and  $D_{45} ID_{45}$  are nonsinusoidal, the resulting current through the parallel connection of these junctions is  $I_s(\varphi) \approx I_c \sin \varphi$  (see Fig. 6) as we observed in experiment. A comparison of absolute value and temperature dependence of  $I_c$  is difficult within the simple model because of the roughness of the interface and consequently the contribution of midgap states is reduced. A distinctive feature of d-wave pairing is the sensitivity of the d-wave superconductor to inhomogeneities and interfaces. Quasiparticle scattering at interfaces distorts the order parameter and causes significant depression of the gap. It happens in the case, when the normal of the interface differs from crystallographic axes even for specularly reflecting boundaries. This phenomenon influences the critical current of the junction as N-layer. Consequently at  $T \approx T_c$ , gap suppression would lead to quadratic dependence of  $I_c(T)$ , which we observed in the experiment (Fig. 2).

In SIS junction, superconducting current is proportional to the transparency of barrier ( $j_c \propto \bar{D}$ ) (see Eq. (1)), since  $R_N S \propto 1/\bar{D}$ , the product  $I_c R_N$  is independent of  $\bar{D}$ . In MSJ, ASJ and symmetrical junction of d-wave superconductor at low  $T$  in a wide range of  $\alpha E_B \propto \sqrt{\bar{D}}$  and as a consequence  $j_c \propto \sqrt{\bar{D}}$  as follows from Eq. (2) and Fig. 5. It happens due to the presence of Andreev's level at  $E \ll \Delta_0$ . The dependence of  $j_c \propto \sqrt{\bar{D}}$  was observed for all out investigated junctions for symmetrical and asymmetrical biasing [15]. The same dependence follows from the data for a symmetrical bicrystal junction on  $\text{SrTiO}_3$  [16].



#### 4. Conclusions

Experimentally observed temperature ( $\propto T$  at  $T < T_c$ ) and transparency ( $\propto \sqrt{D}$ ) dependence of critical current as well as sinusoidal current–phase relation indicate that the transport of superconducting current in high- $T_c$  bicrystal junction possibly realizes by the tunneling of superconducting carrier with participation of bound states at the border caused by multiple Andreev reflection in superconductor with  $d_{x^2-y^2}$  pairing. For a detailed comparison with the theory, the roughness of interface and film twinning should be taken into account.

#### Acknowledgements

The authors thank M. Darula, A. Mashtakov and P.B. Mozhaev for their help with the experiment and fruitful discussions. The work was partially supported by Russia Foundation of Fundamental Research, Russian State Program “Modern Problems of Solid State Physics”, “Superconductivity” division, INTAS program of EU (projects NN97-1940-97-11459) and NATO Scientific program.

#### References

- [1] Koshelets VP, et al. IEEE Trans Appl Supercond 1995;5:3057–60.
- [2] Ovsyannikov GA. In: Groll, Nedkov, editors. Microwave physics techniques. Dordrecht The Netherlands: Kluwer Academic Publishers, 1997. p. 125–40.
- [3] Vale L, et al. IEEE Trans Appl Supercond 1997;7:3193–7.
- [4] Kunkel G, et al. IEEE Trans Appl Supercond 1997;7:3339–42.
- [5] Mashtakov AD, et al. Tech Phys Lett 1999;25:249–54.
- [6] Likharev KK. Rev Mod Phys 1979;51:102–27.
- [7] Barash YS, Galaktionov AV, Zaikin AD. Phys Rev 1995;B52:661–81.
- [8] Kulik IO, Omel'yanchuk AN. Sov J Low Temp Phys 1977;3:459–70.
- [9] Furusaki A, Tsukada M. Phys Rev 1991;B43:10164–9.
- [10] Tanaka Y, Kashiwaya S. Phys Rev 1997;B56:892–912.
- [11] Alff L, et al. Phys Rev 1997;55:R14757–60.
- [12] Barash YuS, Bukrhardt H, Rainer D. Phys Rev Lett 1996;77:4070–3.
- [13] Riedel RA, Bagwell PF. Phys Rev 1998;B57:6084–92.
- [14] Andreev AV, et al. Physica 1994;C226:17–23.
- [15] Ovsyannikov GA et al. Abstract Book of International Conference on Physics and Chemistry of Molecular and Oxide Superconductors. Stockholm, 1999. p. 154.
- [16] Hilgenkamp H, Manhart J. Appl Phys Lett 1998;73:265–7.